END
DATE
FILMED

DTIC

MICROCOPY RESOLUTION TEST CHART

NATIONAL BUREAU OF STANDARDS-1963-A

AD-E301160

DNA-TR-81-79

ON THE MORPHOLOGY OF PLASMA DENSITY IRREGULARITIES IN THE AURORAL F- REGION

James F. Vickrey

5RI International
333 Ravenswood Avenue
Menlo Park, California 94025

1 April 1982

Technical Report

CONTRACT No. DNA 001-81-C-0076

APPROVED FOR PUBLIC RELEASE;
DISTRIBUTION UNLIMITED.

DTIC
ELECTE
AUG 1 1983
S
B

Prepared for
Director
DEFENSE NUCLEAR AGENCY
Washington, DC 20305

83 06 07 050

Destroy this report when it is no longer
needed. Do not return to sender.

SECURITY CLASSIFICATION OF THIS PAGE (When Data Entered)

REPORT DOCUMENTATION PAGE		READ INSTRUCTIONS BEFORE COMPLETING FORM
1 REPORT NUMBER DNA-TR-81-79	2. GOVT ACCESSION NO. *AD-A130930*	3 RECIPIENT'S CATALOG NUMBER
4 TITLE (and Subtitle) ON THE MORPHOLOGY OF PLASMA DENSITY IRREGULARITIES IN THE AURORAL F-REGION		5 TYPE OF REPORT & PERIOD COVERED Technical Report
		6 PERFORMING ORG. REPORT NUMBER SRI Project 2623
7 AUTHOR(s) James F. Vickrey		8 CONTRACT OR GRANT NUMBER(s) DNA 001-81-C-0076
9 PERFORMING ORGANIZATION NAME AND ADDRESS SRI International 333 Ravenswood Avenue Menlo Park, California 94025		10 PROGRAM ELEMENT PROJECT TASK AREA & WORK UNIT NUMBERS Task S99QAXHC-00022
11 CONTROLLING OFFICE NAME AND ADDRESS Director Defense Nuclear Agency Washington, D.C. 20305		12 REPORT DATE 1 April 1982
		13 NUMBER OF PAGES 36
14 MONITORING AGENCY NAME & ADDRESS(if different from Controlling Office)		15 SECURITY CLASS. (of this report) UNCLASSIFIED
		15a DECLASSIFICATION DOWNGRADING SCHEDULE N/A since UNCLASSIFIED

16 DISTRIBUTION STATEMENT (of this Report)

Approved for public release; distribution unlimited.

17 DISTRIBUTION STATEMENT (of the abstract entered in Block 20, if different from Report)

19 KEY WORDS (Continue on reverse side if necessary and identify by block number)

Plasma Density Irregularities
High Latitudes

Propagation Disturbance
Auroral Zone

20 ABSTRACT (Continue on reverse side if necessary and identify by block number)

In this report a framework for understanding the morphology of high latitude plasma density irregularities is developed that has three component parts. Namely, to predict irregularity morphology one must specify (1) the source of irregularities, (2) the lifetimes of irregularities once produced, and (3) the redistribution of irregularities by magnetospheric convection. An irregularity morphology model is developed using the simplest possible source function, classical diffusion, and a simple two-celled magnetospheric

DD FORM 1473 EDITION OF 1 NOV 65 IS OBSOLETE

20. ABSTRACT (Continued)

convection model. While the qualitative results of this model are
encouraging, emphasis is placed on its limitations and how it can be improved
in the future. The motivation for this study is two-fold; first, it is
important to predict the severity of propagation disturbances in the nuclear
disturbed environment. In the absence of actual nuclear data, naturally
occurring auroral disturbances provide a test bed for assessing the accuracy
of predictive codes. Second, naturally occurring plasma density irregulari-
ties hinder DoD communications and surveillance systems. Therefore, under-
standing the processes that control the evolution and ultimate morphology of
naturally structured plasma can help to predict system performance and
perhaps develop mitigants.

TABLE OF CONTENTS

1

LIST OF ILLUSTRATIONS

I INTRODUCTION

The Earth's F-region ionospheric plasma displays structure perpendicular to the magnetic field on scales from hundreds of kilometers down to centimeters. The physical processes that operate over such a wide range of scale sizes are, of course, very diverse. At the largest scales ($\lambda \sim 10$ km), production, loss, and transport of structured plasma are dominated by aeronomic processes including energy sources of magnetospheric origin. At intermediate (0.1 km $< \lambda < 10$ km) and small ($\lambda < 100$ m) scales, plasma instabilities and cross-field plasma diffusion are often the dominant physical processes controlling the plasma structure. However, because nonlinear plasma processes can couple strcutures in one scale length regime to other spatial frequencies, the entire spectrum of irregularities must be studied as a whole.

Polar orbiting satellites find two main zones of maximum irregularity occurrence in the F-layer ionosphere, as detected by both plasma density and electric field fluctuation sensors. One is located near the nighttime magnetic equator. The other zone is located throughout the vast high-latitude region bounded roughly by the polar cusp in the local time zone 0800-1400 and by the equatorial boundary of the high-latitude convection pattern at other local times. This equatorward boundary for the polar zone of structure is thus well equatorward of the classical auroral oval at most local times.

In both of these irregularity zones, the structured plasma can disrupt transionospheric radio wave communication channels. Hence, the interest is practical as well as purely scientific in understanding the processes that control the production, evolution, and decay of plasma structure. The equatorial zone has received the most attention in the recent past in both the theoretical and experimental arenas. This is in part due to the relatively large data base available from radar and rocket measurements made under DNA support at the equator.

3

However, the aeronomic processes are simpler and the sources of free energy capable of driving the F-region plasma dynamics are fewer at the equator than at high latitudes. For example, at mid- and low-latitudes, F-region dynamics are governed principally by neutral atmospheric winds and waves and the dynamo electric field; at high latitudes, these processes are accompanied by particle precipitation, magnetospheric convection electric fields, and auroral current systems flowing parallel and perpendicular to the magnetic field. Nevertheless, the considerable progress made recently in defining and understanding the key physical processes that structure plasma at the equator can also be beneficial to high-latitude studies because many of the processes occurring there (particularly the plasma instabilities) are analogous.

In the next section, we briefly summarize the present understanding of high-latitude plasma structuring phenomena and present a set of working hypotheses that form a framework for investigating the origin and spatial extent of high-latitude irregularities. In the concluding section, we point out the areas for future study that may have the greatest impact on improving this framework. Emphasis is placed on the important contributions that the new DNA polar orbiting satellite, Sondrestrom Radar, and EISCAT may yield.

II MECHANISMS RESPONSIBLE FOR THE OBSERVED MORPHOLOGY OF F-REGION PLASMA STRUCTURE AT HIGH LATITUDES

To predict the observed F-region plasma structure on a global basis, there are three fundamental questions that must be answered:

(1) When and where are plasma density irregularities produced?

(2) How long do they last?

(3) How far do they convect during their lifetime?

A. Irregularity Production

Perhaps the most obvious source of structured plasma at high latitudes is the structured particle precipitation responsible for the aurora. Using satellite data, Dyson and Winningham [1974] showed a one-to-one correlation between the 300 eV electron flux boundary and the penetration of an irregular plasma region. The spatial and temporal structure of incoming precipitation has not yet been examined in sufficient detail (particularly at the low particle energies that produce F-layer ionization) to definitively assess the direct contribution of the spatial spectrum of precipitation to that of the resulting ionization. However, during one rocket flight from Greenland the outer scale of precipitation and plasma density were observed in-situ simultaneously to be ~ 50 km, a value that is similar to that observed in the F-layer ionization enhancements, as measured by incoherent-scatter radar [Kelley et al., 1982]. This agreement suggests that structured soft-particle precipitation is a major source of large-scale F-region plasma density irregularities.

An example of large-scale F-layer density structure, as measured by the Chatanika incoherent-scatter radar, is illustrated in Figure 1, which shows contours of constant electron density as a function of altitude and invariant latitude. The data are displayed in a coordinate

27 FEBRUARY 1980
09.32 TO 09:45 UT

INVARIANT LATITUDE — degrees
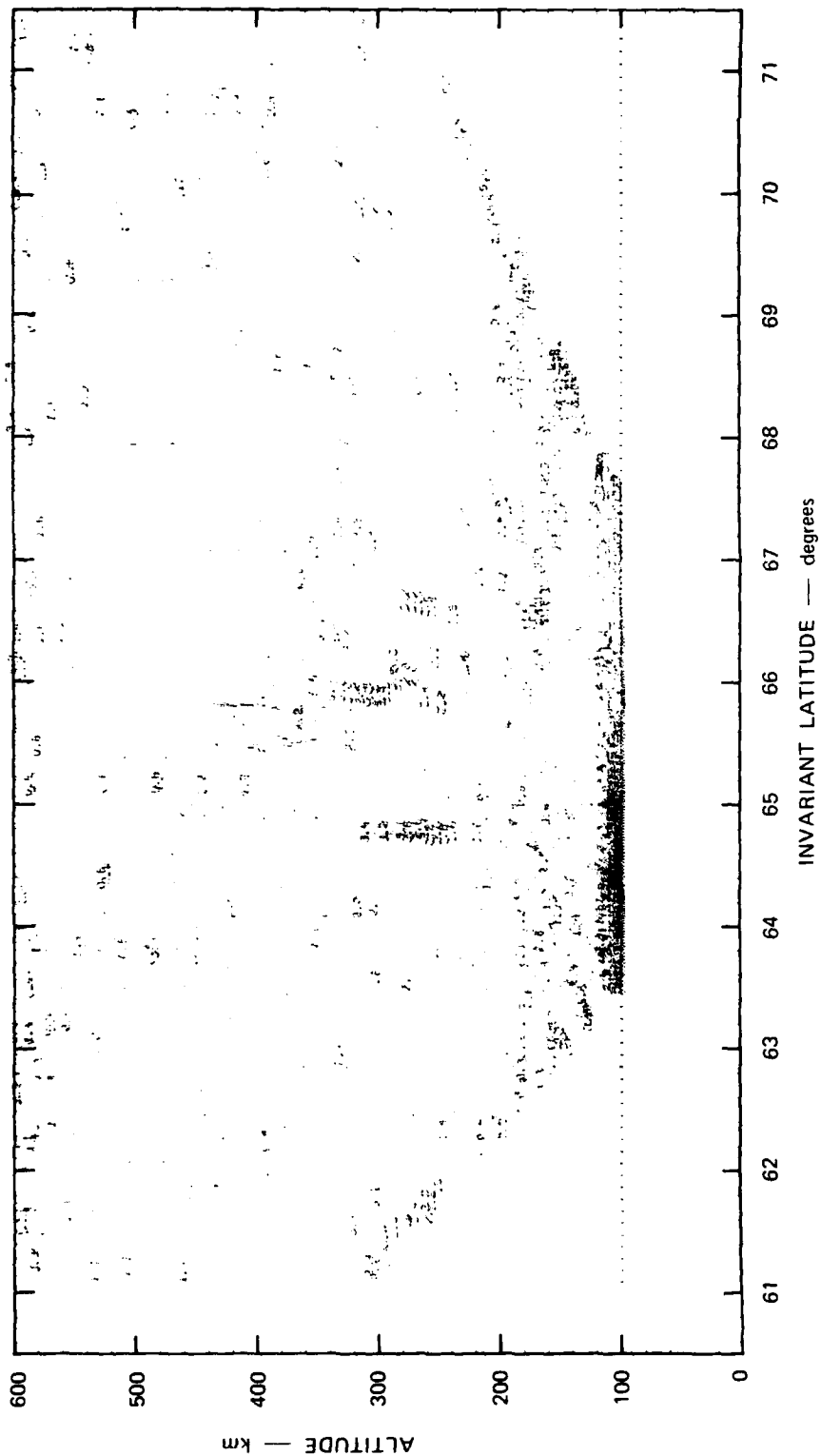
ALTITUDE — km

FIGURE 1   ALTITUDE/LATITUDE VARIATION OF ELECTRON DENSITY IN THE MIDNIGHT-SECTOR AURORAL ZONE MEASURED
BY THE CHATANIKA RADAR

system with straight, vertical magnetic field lines. These observations
from the midnight vector (LT = UT - 10 hours) show F-region ionization
enhancements or plasma "blobs" that reach $\sim 5\text{-}6 \times 10^5$ cm^{-3}, which is
approximately an enhancement by a factor of five over the background.
Plasma-density enhancements ranging from a factor of two to ten over
the background are very commonplace at Chatanika. These blobs are
often observed to convect into the radar field of view from the north
(i.e., following the usual midnight-sector convection pattern) and their
appearance is not necessarily associated with magnetic activity [Vickrey
at al., 1980].

These plasma blobs can be considered analogous to equatorial
"bubbles" because they provide large-scale density gradients upon which
convective plasma instabilities can operate to produce intermediate-
and small-scale plasma structures. Indeed, the steep blob edges are
unstable to the gradient drift instability [Linson and Workman, 1970]
on one side or the other, depending on the local configuration of elec-
tric field and neutral wind. Ossakow and Chaturvedi [1979] have pointed
out that field-aligned currents, which are known to be a permanent
feature of the high latitude ionosphere, are also a destabilizing factor.
Vickrey et al. [1980] combined measurements from the Chatanika radar and
TRIAD satellite to show that the large-scale plasma blobs are linearly
unstable to a generalized form of the $\overline{E} \times \overline{B}$ instability that includes
the effects of field-aligned currents. They also verified the existence
of intermediate-scale plasma structure ($\lambda \approx 1$ km) associated with the
blobs by detecting scintillation enhancements on the TRIAD 150-MHz
telemetry signal. Other evidence for "edge"-related plasma instabili-
ties comes from a rocket flight across an auroral arc [Kelley and
Carlson, 1977; Kelley et al., 1975]. At the edge of the arc intense
(10 mV/m) oxygen ion cyclogron waves were observed as were broadband
short wavelength electrostatic emissions with $k_\perp c_i \approx 1$, where c_i is the
ion gyro radius. Field-aligned currents, perpendicular plasma shear
flow, and parallel sheared-electron flow [Keskinen, private communication,
1982] have all been invoked to explain these waves. Above the arc itself,
the F layer was smooth at these smaller scales.

An important difference between the operation of convective
instabilities at the nighttime equatorial ionosphere and at high
latitudes is the presence of a highly conducting, precipitating-particle-
produced E layer in the auroral zone to which the F-region irregularities
are connected via the geomagnetic field. E-region "shorting" reduces the
growth rate of the convective instabilities and, as will be discussed
more fully below, reduces the lifetime of F-layer irregularities for
scale sizes large enough to map to the E layer [i.e., $\lambda \gtrsim 1$ km; Vickrey
and Kelley (1982)]. However, the presence of the E layer may make it
possible to tap the magnetospheric energy source that might otherwise
not be available.

An additional source of structured plasma density at high latitudes
is the structure in the magnetospheric convection electric field. This
structuring of plasma density can come about in two principal ways.
First, where the electric field is large, there can be a large velocity
difference between ions and neutrals as well as an increase in ion
temperature over the neutral gas temperature because of enhanced Joule
heating. Both of these effects increase the recombination rate of 0^+
with N_2 and result in a change of ion composition of 0^+ to NO^+. Because
the NO^+ recombination rate is relatively large, a density depletion can
occur wherever the electric field is enhanced (i.e., $E \gtrsim 40$ mV/m). Such
effects have been observed at Chatanika [Kelly and Wickwar, 1981].
Although we expect this process to be important only at large scales,
detailed studies of the magnitude of electric field gradients have not
been performed to date.

Second, structured electric fields can produce structured density
by simply mixing flux tubes that have varying plasma density [Fejer and
Kelley, 1980]. A turbulent magnetospheric electric field acting on a
horizontal density gradient can thus produce much the same result as a
local convective instability. Extreme examples of such turbulent fields
are often observed in the winter polar cap during periods of extended
B_z north conditions. (An Example from OGO-6 [Heppner, 1977] is shown in
Figure 2.) No study has been conducted to date, however, regarding the
size of velocity shears normally observed in the lower ionosphere and
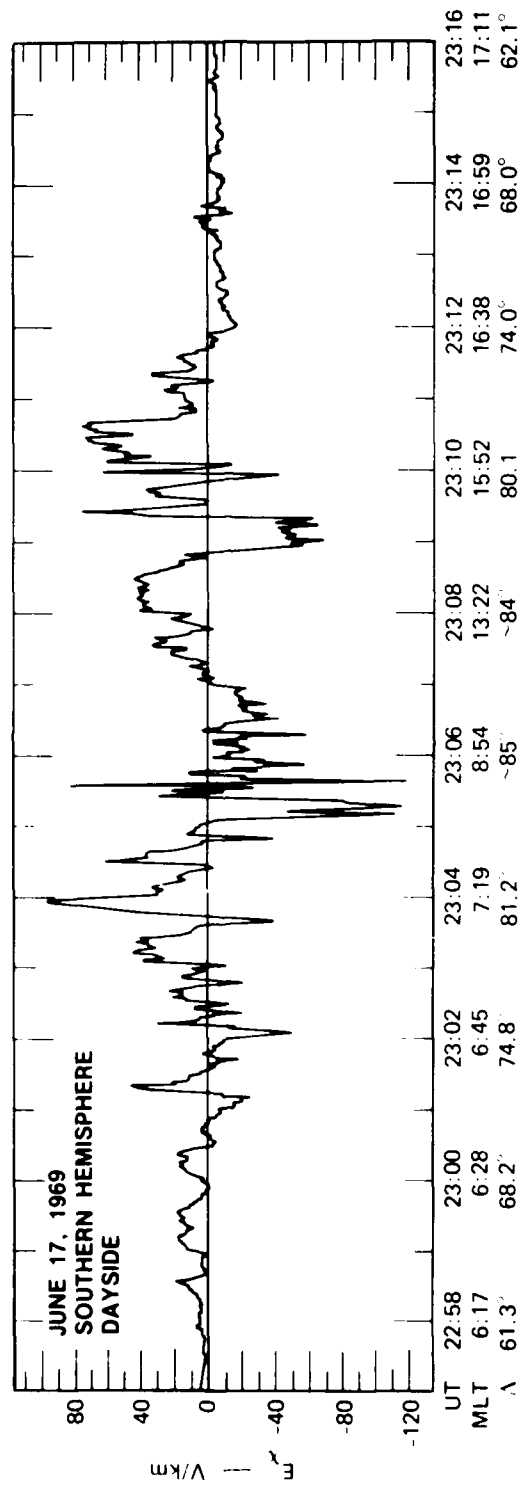
8

FIGURE 2   AN EXAMPLE OF HIGHLY IRREGULAR ELECTRIC FIELDS IN THE DAYSIDE WINTER HEMISPHERE

at what scale sizes they might stir plasma of varying density. Kintner [1976] found shear frequencies (dV/dx) the order of 10^{-1} to 10^{-2} Hz in the upper ionosphere ($\sim$ 2000-km altitude). Mozer et al. [1979] have pointed out that electrostatic shocks are imbedded in regions of intense turbulent electric fields. However, how these map to the F layer is not clear because of the strong evidence for collocated parallel electric fields. Kelley and Carlson [1977] found a shear frequency of 20 Hz in an arc-boundary crossing, but that may be an extreme case.

B. Irregularity Lifetime

The second element in our framework for understanding the morphology of structured plasma at high latitudes is irregularity lifetime. Because we are considering plasma structure in the F layer, recombination will reduce the absolute density on adjacent flux tubes equally (for small amplitude irregularities) and hence, will not reduce horizontal density structure. Thus, the major process governing the removal of F-region plasma density irregularities, once they are produced, is cross-magnetic-field plasma diffusion. A possibly important process that is ignored in the present discussion is the damping of irregularities by convection into a region in which (or a temporal variation resulting in which) the electric field and neutral wind configuration is stabilizing.

The plasma density gradient at the edge of an irregularity has an associated pressure gradient that tends to cause the plasma to diffuse away from regions of more dense plasma and into areas of less dense plasma. The diffusion rate, d_j ($= \rho_j \nu_j$ where ρ_j is the Larmor radius and ν_j is the collision frequency for species j), is larger for ions than for electrons in the F layer because their gyro radius and, hence, their horizontal displacement per collision is much larger than for electrons (even though their collision frequency with neutrals is less than the electron ion collision frequency). However, when the ions try to diffuse away from the electrons, an electrostatic field is produced, which retards ion diffusion. The net result is that the plasma, as a whole, diffuses at twice the slow electron rate.

Let us now consider the effects of a highly conducting auroral E-region, to which the F-layer irregularities may be electrically connected. The electrons in the F layer can easily move along the magnetic field to the E region. In the E region, they participate in horizontal current systems to short out the ambipolar electrostatic field that would otherwise retard ion diffusion. Thus, for a highly conducting E region, classical diffusion proceeds at the ion (rather than the electron) rate. Because ions carry the cross field current and electrons the parallel current, an "image" forms in the E region and acts to slow the net diffusion. However, recombination prevents this for a scale-size λ if $n \gtrsim 10^4/\lambda^2$, where λ is in km and n is in cm^{-3} [Vickrey and Kelley, 1982].

Vickrey and Kelley [1982] have constructed a simple model of classical cross-field plasma diffusion in the F region including E-region conductivity effects. They have found that the cross-field diffusion rate depends strongly on the height of the E and F layers as well as their peak electron densities. The fundamental quantity governing the diffusion rate, however, is the ratio of Pedersen conductivities in the E and F regions, Σ_p^E/Σ_p^F. Figure 3 shows the cross-field diffusion rate, $D_\perp$, and lifetime, $\tau_{1\ km}$, of one-kilometer-scale irregularities [$\tau_\lambda = (\lambda^2/4\pi^2 D_\perp)$] as a function of Σ_p^E/Σ_p^F for typical F-region parameters. The presence of a highly conducting E region can enhance the F-region cross-field plasma diffusion rate by an order of magnitude.

C.   High-Latitude Convection

The final element necessary to explain high-latitude irregularity morphology is convection. Large-scale unstable blobs of plasma such as that shown in Figure 1 are observed to convect with the background electric field [Vickrey et al., 1980]. These large-scale features have very long lifetimes and, thus, can convect far from their origins. Plasma instabilities operating on their edges may produce small-scale plasma structure all along the way. This "cascade" to small scale reduces the lifetime of the large-scale features, but not enough to prevent their transit across the polar cap [Kelley et al., 1982]. This

11
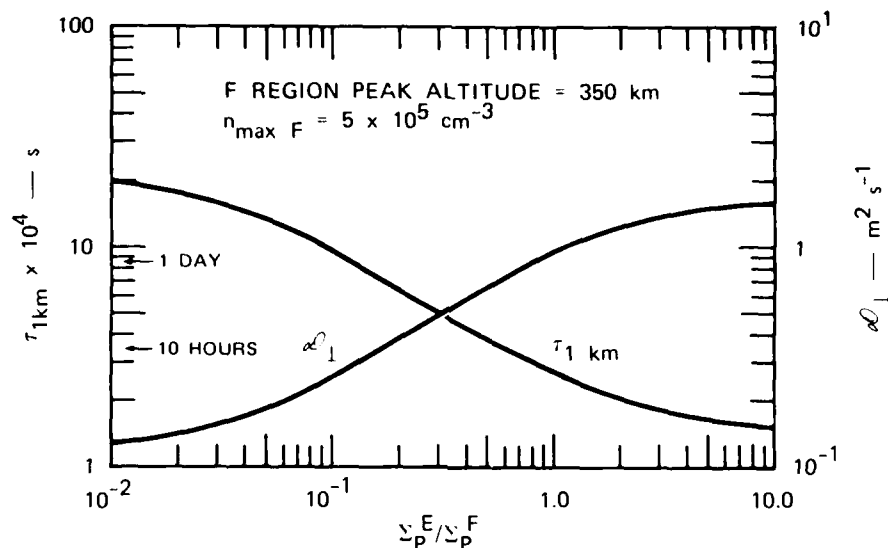
FIGURE 3   THE DEPENDENCE OF CROSS-FIELD DIFFUSION RATE, $D_\perp$, AND LIFETIME OF ONE-km-SCALE IRREGULARITIES, $\tau_{1\ km}$, ON THE RATIO OF E- TO F-REGION PEDERSEN CONDUCTIVITIES

scenario can explain the presence of plasma structure throughout the polar regions of the earth even though "source" regions may be quite localized.

As a framework it is useful to see to what extent a classical aeronomic viewpoint can explain the data. To this end Kelley et al. [1982] have quantified a classical picture of irregularity formation and distribution by combining simple models of irregularity production and loss with a two-celled magnetospheric convection pattern. They considered a simple "source" region of irregularities to be an annular ring near the poleward edge of the auroral oval. This source is a region in which satellites have recorded soft precipitating particle fluxes [Foster and Burrows, 1976; Hardy, private communication]. The irregularity lifetime was calculated using the classical diffusion model of Vickrey and Kelley [1982], which includes E-region conductivity effects. The global E-region conductivity distribution assumed was that given by Spiro et al., [1978]. Figure 4 shows the results obtained by Kelley et al., [1982]. The trajectories (in the inertial frame) of four flux tubes across the polar cap and around the auroral zone are shown. The numbers indicate the amplitude in dB of one-kilometer-scale irregularities, $|\Delta N/N|^2$, where N is electron density. The amplitude is

12

AMPLITUDE $\frac{\Delta N}{N}^2$

NOON

-14
-12
0
-1
0
-22
0
-10
50
60
70
-4
-2
-10
WINTER
SOLSTICE
-2
-2
-20
DUSK
-6
-2
-4
DAWN
2
-6
350 km
SHADOW
HEIGHT
0
-10
-20
80
-6
-8
0
-8
-8
-10
0
-6
EQUINOX
0
-4
0
-16
10
-4
4
0
-8
-2

MIDNIGHT
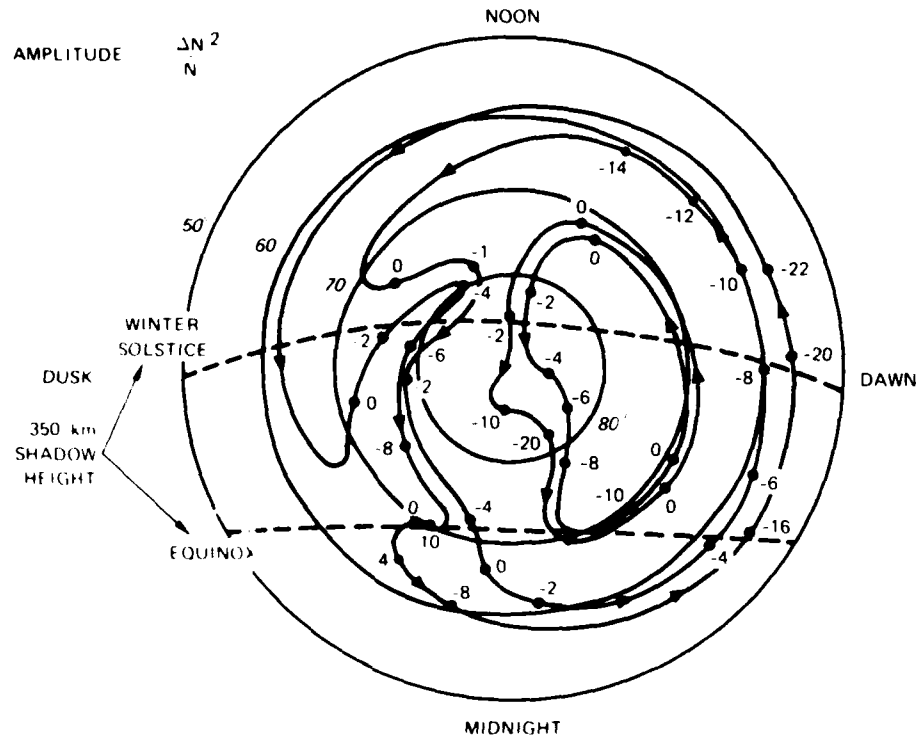
FIGURE 4   ILLUSTRATION OF THE LATITUDE AND LOCAL-TIME VARIATIONS
(IN THE INERTIAL FRAME) OF THE AMPLITUDE (IN dB) OF ONE-
km-SCALE ELECTRON DENSITY IRREGULARITIES

reset to 0 dB whenever the trajectories cross the source region near
the poleward edge of the auroral oval. A similar plot for 10-km
structures would show almost negligible decay, because diffusion acts
100 times more slowly at that scale size.

Figure 5 is a similar plot that includes the overall decay of the
ionosphere because of recombination, which reduces the irregularity and
background density by approximately 4 dB per hour of travel time. This
plot, then, is more representative of the spectral strength $|\Delta N|^2$;
hence, it is perhaps more descriptive of scintillation effects. The
peak F-region density is assumed 5×10^5 cm^{-3} in the production zone,
with the density maximum at a height of 350 km. A Chapman layer is
also assumed [Vickrey and Kelley, 1982]. Winter conditions are taken

13
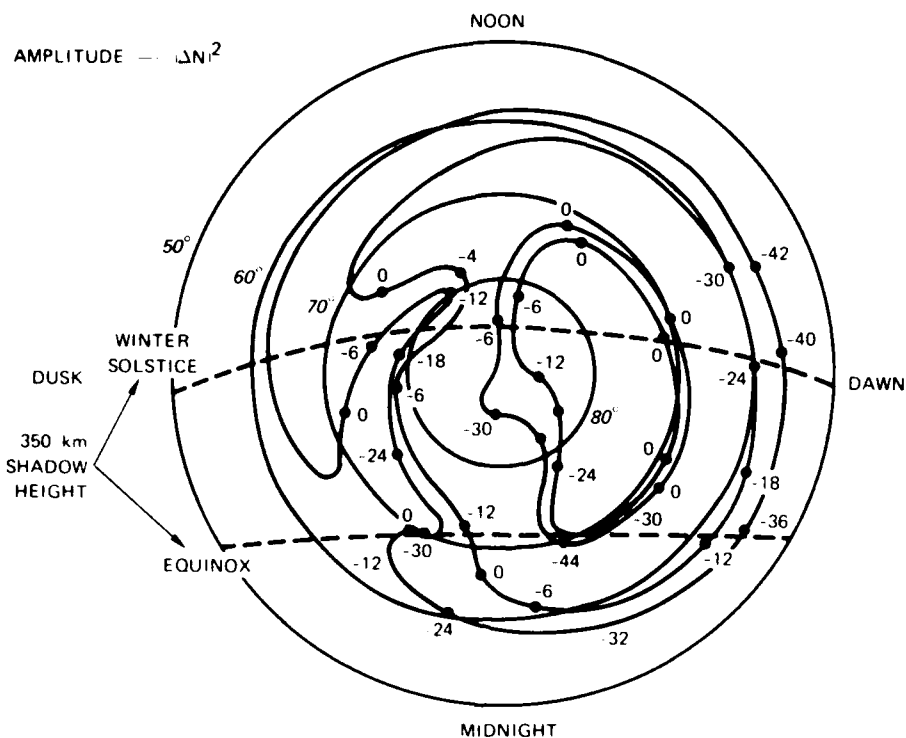
FIGURE 5   ILLUSTRATION OF THE LATITUDE AND LOCAL-TIME VARIATIONS
(IN THE INERTIAL FRAME) OF THE AMPLITUDE (IN dB) OF ONE-
km-SCALE ELECTRON DENSITY IRREGULARITIES INCLUDING THE
EFFECTS OF RECOMBINATIONAL DECAY

so as to emphasize the effects of auroral production and decay.   A
dashed line marks the terminator at 350-km altitude during winter and
equinox.   When the absolute density decayed to 5×10^3 cm^{-3}, the recom-
bination decay was stopped.   In such a case, the assumption of an 0^+
plasma is no longer valid, and longer-lived ions may dominate the F_2
layer composition [Heelis et al., 1981].

Despite the simplicity of this first attempt to assess the relative
roles of production, convection, and decay in determining high-latitude
irregularity morphology, this model leads to a number of useful conclu-
sions.   For example, 10-km size density fluctuations can survive transport
throughout the polar cap and auroral zone if sunlight does not illuminate

14

the region for a prolonged period and fill in the background. At one-kilometer scale, the classical diffusion discussed here and in Vickrey and Kelley [1982] has a significant effect in some regions of the polar cap and auroral zone. For example, a very deep irregularity "hole" can be formed in the central polar cap, as experimentally reported by Kelley and Mozer [1972]. This is primarily due to the long time that a flux tube can spend in the central polar region. Even in the 10-km case, a very sharp gradient in irregularity intensity is formed at the equatorward edge of the nighttime magnetospheric-convection zone--not the auroral oval. This agrees excellently with many studies of the high-latitude irregularity boundary [see review by Fejer and Kelley, 1980]. However, other sources of plasma density irregularities, such as mid-latitude spread F and processes associated with plasma density gradients near the F-region trough can also contribute to irregularity formation at times.

In relatively quiet times, the postsunset local-time region, 1800 to 2100, between 60° and 68° should not contain many irregularities because, in the nonrotating frame, flux tubes only enter this region from the sunlit sector. For the same reason, the equatorward boundary of the irregularity zone should be at higher latitudes in the dusk sector than in the dawn sector, to which midnight-sector auroral-oval irregularities can rapidly convect. This agrees with the ISIS results reported by Sagalyn et al., [1974], who showed that the boundary was about 3° higher in latitude in the dusk sector for $K_p \leq 3$. The difference was less pronounced for $K_p > 3$. This is reasonable because, with increasing magnetic activity, large convection speeds can dominate over the corotation velocity at lower latitudes in the local time sector near and just after dusk.

Note that, although the source function would be much different from that used to construct Figure 5, the high-density debris from a nuclear exchange would at late times eventually be transported and distributed in accordance with this flow pattern. The extremely long lifetimes expected for the structured plasma could, thus, impact on DoD communications and surveillance systems at great distances from, and for long periods after a detonation.

15

We turn now to ways in which the classical model does not fit the
observations. Figure 6 shows the average electric field strength at
31 Hz (~ 200-m scale fluctuations) measured by the OV1-17 satellite
[Kelley and Mozer, 1972] as a function of invariant latitude. Note
that the irregularity amplitude has a latitudinal trend that is qual-
itatively similar to that expected from Figures 4 and 5 in a noon-to-
midnight cross section. Namely, there is a strong source of irregu-
larities in the polar cusp, a decay of irregularity amplitude in the
central polar cap, and another source region in the midnight-sector
auroral oval. These observations make it apparent, however, that the
simple model illustrated in Figures 4 and 5 grossly misrepresents the
amplitude of small-scale irregularities; for example, the decrease in
amplitude for 200-m scales in Figures 4 and 5 should be multiplied by
a factor of 25. However, the amplitude decrease actually observed
across the polar cap for 200-m scales is even less than that expected
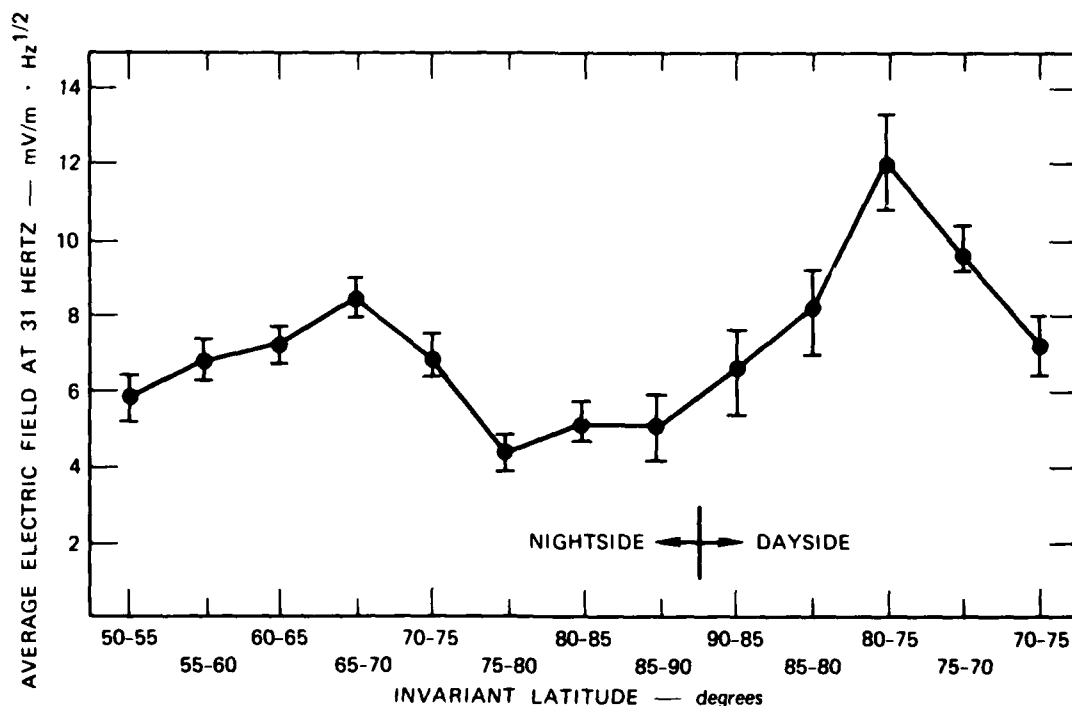for kilometer-scale structures. These data thus suggest that intermediate-

FIGURE 6   AVERAGE ELECTRIC-FIELD STRENGTH AT 200-m SCALE AS A FUNCTION OF
            LATITUDE

16

and small-scale irregularities are continuously generated throughout the polar cap, probably on the unstable edges of the larger-scale blobs. As mentioned above, such a cascade process would hasten the removal of large-scale features, but not enough to prevent their transit through the polar cap.

It is interesting to turn the problem around by interpreting Figure 6 in terms of anomalous diffusion at large scales. This can be done as follows: Suppose the irregularity spectrum $S(k) = |\Delta N(k)|^2$, has a rigid shape (e.g., $S(k) \propto k^{-2}$) as a set of adjacent flux tubes convect across the polar cap. Then, the decrease in amplitude of 200-m irregularities reflects a decrease in energy stored at the input scale, which is of order $\lambda \approx 10$ km. The quasi-exponential spatial decrease in irregularity amplitude in Figure 6 between $75°$ invariant latitude on the dayside cusp and $75°$ on the nightside can be converted to an effective diffusion rate, D_{eff}, if we assume the average antisunward drifts from the Spiro et al. [1978] convection model. This exercise leads to an effective diffusion rate that is within ~ 60 percent of the Bohm diffusion rate measured empirically in laboratory plasmas. This D_{eff} is approximately 100 times faster than the classical diffusion rate.

The above calculation is obviously too approximate and based on too many unverified assumptions to prove conclusively that the Bohm diffusion process is operating in the polar cap. Nonetheless, it strongly suggests that some anomalous process is operating that is much faster than classical diffusion. To proceed in the future, it will be necessary to measure the complete spectrum of irregularities and their associated electric fields across the polar regions to distinguish between anomalous diffusion processes due to various microinstabilities [e.g., Gary, 1980]. This will be discussed more fully in Section III.

D. Irregularity Geometry

Any viable theory for the formation and evolution of plasma structure must ultimately account for the observed geometry of plasma density irregularities. Auroral-zone scintillation measurements from

the Wideband satellite show enhancements in scintillation whenever the propagation vector lies in the _plane_ of the local L-shell, not just when it coincides with the local magnetic field _line_. This phenomenon suggests that the intermediate-scale ($\sim$ 1 km) irregularities responsible for the scintillation are L-shell-aligned sheet-like structures rather than simple rods. This unexpected geometry has been confirmed by spaced-receiver scintillation measurements in the midnight sector auroral zone. These measurements show a high ratio (up to 10 to 1) of spatial coherence in the magnetic east-west direction as compared to the north-south direction [Rino et al., 1978]. The linear gradient drift and current convective instabilities operating on the meridional density gradients shown in Figure 1 tend to produce irregularities with a $\hat{k}$ vector in the east-west plane; i.e., orthogonal to the geometry of the kilometer-scale structures that is actually observed. This apparent paradox has been addressed by Chaturvedi and Ossakow [1972a, b], whose analysis shows that the linearly unstable mode of the gradient drift and current convective instabilities can transfer energy through nonlinear coupling to a (linearly stable) mode whose wave vector lies in the plane of the density gradient.

Recently, Keskinen and Ossakow [1982] have performed numerical simulations of the gradient drift and current convective instabilities operating on a blob such as shown in Figure 1 for typical auroral F-region conditions. They have found that the primary and associated (secondary) small-scale structures can be oriented in either the north-south or east-west direction depending on the ambient electric field magnitude and direction. Because the meridional electric-field component in the auroral zone is typically five times the zonal component, any primary (north-south) structure can be quickly destabilized by the meridional electric-field component to produce secondary structure, which is east-west aligned.

Another mechanism for producing kilometer-scale east-west structures in the auroral zone can result if the large-scale blobs themselves are not infinitely extended in the east-west direction. Any large-scale zonal gradients can be acted upon by the meridional

18

electric field to produce (primary) east-west aligned structure. Recently, a campaign of experiments with the Chatanika radar was conducted to measure east-west structure of the large-scale blobs. The preliminary results from those experiments indicate that although the *east-west scale lengths can be very much longer than those north-south* (particularly during magnetically quiet times), there are also occasions when the east-west extent of the blobs is comparable to the meridional extent (Tsunoda, private communication).

Another process that might explain the observed anisotropy of medium-scale irregularities at high latitudes is the behavior of an incompressible fluid in a sheared convective-flow pattern. A very simple example is illustrated schematically in Figure 7. The situation was constructed to be similar to the premidnight sector convective flow pattern out of the polar cap, where flow is principally sun-aligned, and into the auroral oval, where flow is principally zonal. An irregularity represented by the ellipsoid contour of constant electron density was chosen to be initially sun aligned (i.e., perpendicular to what is
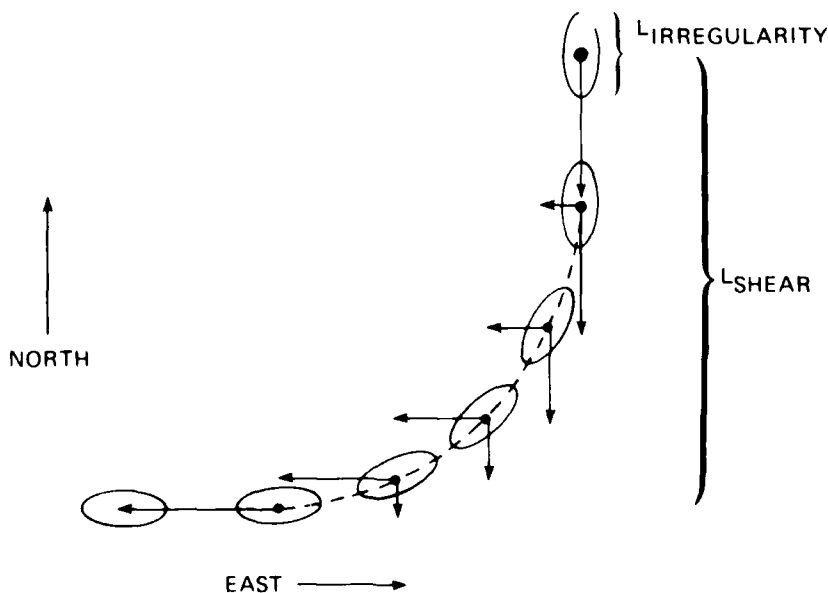

FIGURE 7   SCHEMATIC ILLUSTRATION OF AN ANISOTROPIC IRREGULARITY SUBJECTED TO A SHEARED FLOW PATTERN

19

observed in the auroral zone). Because the F region plasma is incompressible, the area of the ellipsoid remains constant. The equatorward tip of the irregularity enters the region of westward flow before the poleward tip. Therefore, the irregularity becomes either kinked or smoothly rotated (depending on the ratio of irregularity size, $L_{irregularity}$, to shear (or rotation) size, L_{shear}) as it drifts further south. In general, however, we expect the irregularity to be aligned with the streamlines of flow. Thus this model predicts east-west aligned sheets in the auroral oval except perhaps very near the Harang discontinuity. It is interesting to note that a conservative velocity shear (given by assuming that a 500 m/s meridional flow in the polar cap changes to a 500 m/s westward flow in the auroral oval over a meridional distance of 500 km) is on the order of 10^{-3} Hz. This value is comparable to the $\overline{E} \times \overline{B}$ instability growth rates observed by Vickrey et al. [1980] for an unstable blob. Thus, by the time an irregularity has formed, it should already be rotated to align with flow lines.

Evidence that convection may indeed influence irregularity geometry can be found in the latitude-local time variations of anisotropy determined from spaced receiver scintillation measurements. Figure 8 shows the preliminary results of such a compilation (R. C. Livingston, private communication) for Wideband Satellite passes recorded at Poker Flat, Alaska (65° invariant latitude, Local Time = UT - 10 hours) during February and March of 1978. The data show a dramatic change in kilometer scale irregularity anisotropy between the polar cap where irregularities appear to be isotropic or rod-like depending on local time and lower latitudes where irregularities can be sheet-like throughout the evening. Note that the elongation of the sheets and rods is reduced in the midnight sector (i.e., near the Harang discontinuity). One possible reason why the polar cap irregularities appear to be isotropic or rod-like may be that the winter polar cap flow is very irregular. A similar analysis of summer polar cap data (where flow is expected to be more regular) is underway.
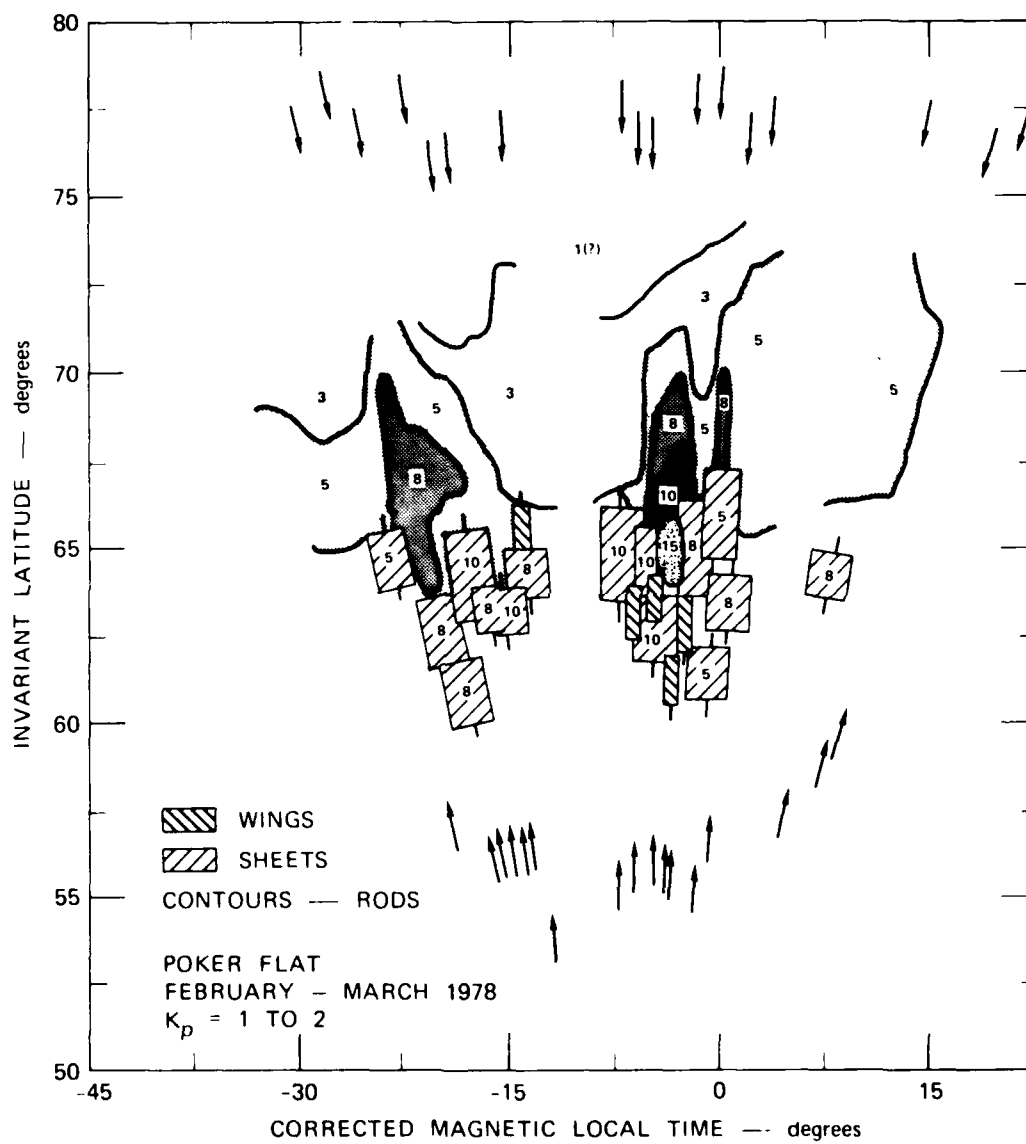
FIGURE 8   LATITUDE-LOCAL-TIME VARIATION OF IRREGULARITY ANISOTROPY

III FUTURE RESEARCH

Our framework for understanding high-latitude irregularity
morphology consists of three simple component parts--irregularity
production, transport, and decay. It is clear, however, that none
of these component parts is well understood at present. Indeed,
fundamental questions remain in each area that can be addressed by
the new DNA satellite, the Sondrestrom Radar, and EISCAT.

In the area of irregularity production, the source regions of
large-scale blobs are known to be much more complicated than the
simple ring used in the model of Kelley et al. [1982]. For example,
sun-aligned F layer polar cap arcs are known to be a strong source
of radio wave scintillation [Weber and Buchau, 1980] and thus should
be included in the "source function." This large-scale source function
can be better defined by analyzing data from precipitating-particle
detectors aboard polar-orbiting satellites and perhaps from satellite
imaging. These measurements should be augmented by ground-based
incoherent-scatter measurements that can probe the three-dimensional
density structure that results from this precipitation. It is impor-
tant that the particle detector have a high spatial resolution because
at present the nature of the spatial spectrum of soft precipitation
is unknown. For example, can structured precipitation directly produce
structured ionization at kilometer scales and smaller or is precipita-
tion only responsible for large-scale "seed" features upon which
instabilities operate? Because the E-region conductivity produced
by energetic precipitation is an important consideration for both the
growth rate of convective instabilities and for the lifetime of ir-
regularities once they are produced, the particle detector should also
be sensitive to high energies so that the global conductivity pattern
can be modeled.

It has been shown that convective plasma instabilities are operative in the high-latitude ionosphere. However, they have many important properties that merit further examination. For example, it is now becoming clear that the spectrum of irregularities present on a given flux tube of plasma depends in a complicated way on the past history of that flux tube. Thermal diffusion operates slowly as compared to observed instability growth rates. Thus, instability growth is, to some extent, cumulative as a flux tube convects between unstable and benign regions. Therefore, to predict the amount of plasma structure at a given point, the minimum destabilizing influences a flux tube has encountered in crossing the polar regions must be assessed. These influences include the magnitude and direction of the electric field and neutral wind with respect to the density gradient as well as the amplitude of the field-aligned current, which is known to be a permanent feature of the auroral zone. Measurement of the latter can be performed by a satellite-borne vector magnetometer; however, detailed knowledge of the neutral wind pattern at high-latitudes requires more extensive ground-based optical measurements as well as improved modeling. Simultaneous in-situ measurement of δE and $\delta n/n$ should help separate the various instability mechanisms. This has been used successfully at the magnetic equator to identify drift waves as an important contributor to the cascade of energy from long to short scales [Kelley et al., 1982].

High-latitude convection can be measured by polar orbiting satellites with electric-field detectors as well as by incoherent-scatter radar. It is important to further characterize the global changes in this pattern caused by variations in the interplanetary magnetic field and solar wind conditions. Moreover, high spatial-resolution electric-field measurements are required to determine the magnitude of velocity shears. Furthermore, small-scale waves that are thought to play a role in anomalous diffusion (which may in turn be the controlling factor determining irregularity lifetime) can be detected and studied. For example, in the equatorial case, it has been shown that waves of the drift-mode type are more easily detected

23

through their electric-field signatures and that the wave type can be identified through comparisons of δE and $\delta n/n$ [Kelley et al., 1982]. Other crucial elements in the study of anomalous diffusion are to measure the entire spectrum of density structure from hundreds of kilometers to meters, if possible, and to document spectral changes between the polar cap, auroral zone, and trough.

The complicated geometry of plasma density irregularities is an interesting area for further research. Whether this geometry is the result of precipitation structure, nonlinear saturation of a convective instability, a secondary instability, or simply a result of convective flow patterns is an open question. Certainly the answer will depend upon the scale size of interest. At large scales, combined ground-based optical and incoherent-scatter radar measurements may shed some light on the answer. At intermediate and small scales, further spaced-receiver scintillation measurements are required.

REFERENCES

Chaturvedi, P. K., and Ossakow, S. L., "Nonlinear Stabilization of the E × B Gradient Drift Instability in Ionospheric Plasma Clouds," J. Geophys. Res., Vol. 84, No. A2, p. 419 (February 1979).

Chaturvedi, P. K., and Ossakow, S. L., "Nonlinear Stabilization of the Current Convective Instability in the Diffuse Aurora," J. Geophys. Letts., Vol. 6, No. 12, p. 957 (December 1979).

Dyson, P. L., and Winningham, J. D., "Topside Ionospheric Spread F and Particle Precipitation in the Dayside Magnetospheric Clefts," J. Geophys. Res., Vol. 79, p. 5219 (1974).

Fejer, B. G., and Kelley, M. C., "Ionospheric Irregularities," Rev. Geophys. and Space Sci., Vol. 18, No. 2, p. 401 (May 1980).

Foster, J. C. and Burrows, J. R., "Electron Fluxes Over the Polar Cap: 1. Intense KeV Fluxes During Post-Storm Quieting," J. Geophys. Res., Vol. 81, No. 34, p. 6016 (December 1976).

Gary, S. P., "Wave Particle Transport From Electrostatic Instabilities," Phys. Fluids, Vol. 23, No. 6, p. 1193 (June 1980).

Heelis, R. A., Murphy, J. A., and Hanson, W. B., "A Feature of the Behavior of He^+ in the Nightside High-Latitude Ionosphere During Equinox," J. Geophys. Res., Vol. 86, No. A1, p. 59 (January 1981).

Heppner, J. P., "Empirical Models of High-Latitude Electric Fields," J. Geophys. Res., Vol. 82, No. 7, p. 1115 (March 1977).

Kelley, M. C., and Carlson, C. W., "Observation of Intense Velocity Shear and Associated Electrostatic Waves Near an Auroral Arc," J. Geophys. Res., Vol. 82, p. 2343 (1977).

Kelley, M. C., and Mozer, F. S., "A Satellite Survey of Vector Electric Fields in the Ionosphere at Frequencies of 10-500 Hz: 1. Isotropic, High-Latitude Electrostatic Emissions," J. Geophys. Res., Vol. 77, No. 22, p. 4158 (August 1972).

Kelley, M. C., Bering, C. E., and Mozer, F. S., "Evidence That the Ion Cyclotron Instability is Saturated by Ion Heating," _Phys. Fluids_, Vol. 18, p. 1590 (1975).

Kelley, M. C., Vickrey, J. F., Carlson, C. W., and Torbert, R., "On the Origin and Spatial Extent of High-Latitude F-region Irregularities," _J. Geophys. Res._, in press.

Kelley, M. C., Pfaff, C. R., Baker, K. D., Ulwick, J. C., Livingston, R. C., Rino, C. L., and Tsunoda, R. T., "Simultaneous Rocket Probe and Radar Measurements of Equatorial Spread F--Transitional and Short Wavelength Results," submitted to _J. Geophys. Res._

Kelly, J. D., and Wickwar, V. B., "Radar Measurements of High-Latitude Ion Composition Between 140 and 300-km Altitude," _J. Geophys. Res._, Vol. 86, No. A9, p. 7617 (September 1981).

Keskinen, M. J., and Ossakow, S. L., "Nonlinear Evolution of Plasma Enhancements in the Auroral Ionosphere: 1. Long Wavelength Irregularities," _J. Geophys. Res._, Vol. 87, p. 144 (January 1982).

Kintner, P. M., "Observations of Velocity Shear Driven Plasma Turbulence," _J. Geophys. Res._, Vol. 81, p. 5114 (1976).

Linson, L. M. and Workman, J. B, "Formation of Striations in Ionospheric Plasma Clouds," _J. Geophys. Res._, Vol. 75, No. 16, p. 3211 (June 1970).

Mozer, F. S., Cattell, C. A., Temerin, M., Torbert, R. B., Vonglinski, S., Woldorf, M., and Wygant, J., "The dc and ac Electric Field, Plasma Density, Plasma Temperature, and Field-Aligned Current Experiments on the S3-3 Satellite," _J. Geophys. Res._, Vol. 84, No. A10, p. 5875 (1979).

Ossakow, S. L., and Chaturvedi, P. K., "Current Convective Instability in the Diffuse Aurora," _Geophys. Res. Letts._, Vol. 6, No. 4, p. 322 (April 1979).

Rino, C. L., Livingston, R. C., and Matthews, S. J., "Evidence for Sheet-Like Auroral Ionospheric Irregularities," _Geophys. Res. Letts._, Vol. 5, No. 12, p. 1034 (December 1978).

Sagalyn, R. S., Smiddy, M., and Ahmed, M., "High-Latitude Irregularities in the Topside Ionosphere Based on ISIS 1 Thermal Probe," _J. Geophys. Res._, Vol. 79, No. 28, p. 4253 (October 1974).

Spiro, R. W., Heelis, R. A., and Hanson, W. B., "Ion Convection and the Formation of the Mid-Latitude F-region Ionization Trough," _J. Geophys. Res._, Vol. 82, No. A9, p. 4255 (September 1978).

Vickrey, J. F., and Kelley, M. C., "The Effects of a Conducting E layer on Classical F-region Cross-Field Plasma Diffusion," submitted to _J. Geophys. Res._

Vickrey, J. F., Rino, C. L., and Poterma, T. A., "Chatanika/Triad Observations of Unstable Ionization Enhancements in the Auroral F region," _Geophys. Res. Letts._, Vol. 7, No. 10, p. 789 (October 1980).

Wallis, D. D., and Budzinski, E. E., "Empirical Models of Height-Integrated Conductivities," _J. Geophys. Res._, Vol. 86, No. A1, p. 125 (January 1981).

Weber, E. J., and Buchau, J., "Polar Cap F-layer Auroras," _Geophys. Res. Letts._, Vol. 8, No. 1, p. 125 (January 1980).

DEPARTMENT OF DEFENSE

Assistant to the Secretary of Defense
Atomic Energy
        ATTN: Executive Assistant

Command & Control Technical Center
        ATTN: C-650
        ATTN: C-312, R. Mason
        ATTN: C-650, G. Jones
 3 cy ATTN: C-650, W. Heidig

Defense Communications Agency
        ATTN: Code 230
        ATTN: Code 205
        ATTN: J300 for Yen-Sun Fu

Defense Communications Engineer Center
        ATTN: Code R410, N. Jones
        ATTN: Code R410
        ATTN: Code R410, R. Craighill
        ATTN: Code R123

Defense Intelligence Agency
        ATTN: DB-4C, E. O'Farrell
        ATTN: DC-7B
        ATTN: DB, A. Wise
        ATTN: DT-1B
        ATTN: DIR

Defense Nuclear Agency
        ATTN: STNA
        ATTN: NAFD
        ATTN: RAEE
        ATTN: NATD
        ATTN: RAAE, P. Lunn
 3 cy ATTN: RAAE
 4 cy ATTN: TITL

Defense Technical Information Center
12 cy ATTN: DD

Dep Under Secretary of Defense
Comm, Cmd, Cont & Intell
        ATTN: Dir of Intelligence Sys

Field Command
Det 1, Defense Nuclear Agency
Lawrence Livermore Lab
        ATTN: FC-1

Field Command
Defense Nuclear Agency
        ATTN: FCPR
        ATTN: FCTXE
        ATTN: FCTT, G. Ganong
        ATTN: FCTT, W. Summa

Interservice Nuclear Weapons School
        ATTN: TTV

Joint Chiefs of Staff
        ATTN: C3S
        ATTN: C3S, Evaluation Office (HDOO)

DEPARTMENT OF DEFENSE (Continued)

Joint Strat Tgt Planning Staff
        ATTN: JLA, Threat Applications Div
        ATTN: JLTW-2

National Security Agency
        ATTN: W-32, O. Bartlett
        ATTN: R-52, J. Skillman
        ATTN: B-3, F. Leonard

Under Secy of Def for Rsch & Engrg
        ATTN: Strategic & Space Sys (OS)
        ATTN: Strat & Theater Nuc Forces, B. Stephan

WWMCCS System Engineering Org
        ATTN: J. Hoff

DEPARTMENT OF THE ARMY

Assistant Chief of Staff for Automation & Comm
        ATTN: DAMO-C4, P. Kenny

Atmospheric Sciences Laboratory
        ATTN: DELAS-EO, F. Niles

BMD Advanced Technology Center
        ATTN: ATC-R, D. Russ
        ATTN: ATC-O, W. Davies
        ATTN: ATC-R, W. Dickinson
        ATTN: ATC-T, M. Capps

BMD Systems Command
        ATTN: BMDSC-HLE, R. Webb
 2 cy ATTN: BMDSC-HW

Deputy Chief of Staff for Ops & Plans
        ATTN: DAMO-RQC, C2 Div

Harry Diamond Laboratories
        ATTN: DELHD-NW-P
        ATTN: DELHD-NW-R, R. Williams

US Army Chemical School
        ATTN: ATZN-CM-CS

US Army Comm-Elec Engrg Instal Agency
        ATTN: CCC-EMEO-PED, G. Lane
        ATTN: CCC-CED-CCO, W. Neuendorf

US Army Communications Command
        ATTN: CC-OPS-W
        ATTN: CC-OPS-WR, H. Wilson

US Army Communications R&D Command
        ATTN: DRDCO-COM-RY, W. Kesselman

US Army Foreign Science & Tech Ctr
        ATTN: DRXST-SD

US Army Materiel Dev & Readiness Cmd
        ATTN: DRCLDC, J. Bender

DEPARTMENT OF THE ARMY (Continued)

US Army Nuclear & Chemical Agency
    ATTN: Library

US Army Satellite Comm Agency
    ATTN: Document Control

US Army TRADOC Sys Analysis Actvy
    ATTN: ATAA-PL
    ATTN: ATAA-TCC, F. Payan, Jr
    ATTN: ATAA-TDC

USA Missile Command
    ATTN: DRSMI-YSO, J. Gamble

DEPARTMENT OF THE NAVY

Joint Cruise Missiles Project Ofc
    ATTN: JCMG-707

Naval Air Systems Command
    ATTN: PMA 271

Naval Electronic Systems Command
    ATTN: PME 117-211, B. Kruger
    ATTN: PME 106-13, T. Griffin
    ATTN: Code 501A
    ATTN: PME 117-20
    ATTN: PME 117-2013, G. Burnhart
    ATTN: Code 3101, T. Hughes
    ATTN: PME 106-4, S. Kearney

Naval Intelligence Support Ctr
    ATTN: NISC-50

Naval Ocean Systems Center
    ATTN: Code 5322, M. Paulson
    ATTN: Code 532
    ATTN: Code 5323, J. Ferguson

Naval Research Laboratory
    ATTN: Code 4720, J. Davis
    ATTN: Code 4780
    ATTN: Code 7500, B. Wald
    ATTN: Code 4780, S. Ossakow
    ATTN: Code 6700
    ATTN: Code 7950, J. Goodman
    ATTN: Code 4187
    ATTN: Code 4700

Naval Space Surveillance System
    ATTN: J. Burton

Naval Surface Weapons Center
    ATTN: Code F31

Naval Telecommunications Command
    ATTN: Code 341

Ofc of the Deputy Chief of Naval Ops
    ATTN: OP 981N
    ATTN: OP 941D
    ATTN: NOP 654, Strat Eval & Anal Br

Office of Naval Research
    ATTN: Code 412, W. Condell
    ATTN: Code 414, G. Joiner

DEPARTMENT OF THE NAVY (Continued)

Strategic Systems Project Office
    ATTN: NSP-2141
    ATTN: NSP-2722, F. Wimberly
    ATTN: NSP-43

Theater Nuclear Warfare Prj Office
    ATTN: PM-23, D. Smith

DEPARTMENT OF THE AIR FORCE

Aerospace Defense Command
    ATTN: DC, T. Long

Air Force Geophysics Laboratory
    ATTN: OPR, H. Gardiner
    ATTN: OPR-1
    ATTN: LKB, K. Champion
    ATTN: CA, A. Stair
    ATTN: PHY, J. Buchau
    ATTN: R. Babcock
    ATTN: R. O'Neil

Air Force Technical Applications Ctr
    ATTN: TN

Air Force Weapons Laboratory
    ATTN: SUL
    ATTN: NTYC
    ATTN: NTN

Air Force Wright Aeronautical Lab
    ATTN: A. Johnson
    ATTN: W. Hunt

Air Logistics Command
    ATTN: OO-ALC/MM

Air University Library
    ATTN: AUL-LSE

Assistant Chief of Staff
Studies & Analyses
    ATTN: AF/SASC, C. Rightmeyer
    ATTN: AF/SASC, W. Kraus

Ballistic Missile Office
    ATTN: ENSN, W. Wilson
    ATTN: SYC, Col Kwan

Deputy Chief of Staff
Research, Development, & Acq
    ATTN: AFRDS, Space Sys & C3 Dir
    ATTN: AFRDSS
    ATTN: AFRDSP

Deputy Chief of Staff
Operations and Plans
    ATTN: AFXOICD
    ATTN: AFXOKT
    ATTN: AFXOKS

Electronic Systems Div
    ATTN: SCT-2, J. Clark

Electronic Systems Division
    ATTN: XRT-2, J. Deas

DEPARTMENT OF THE AIR FORCE (Continued)

Electronic Systems Division
    ATTN: SCS-1E
    ATTN: SCS-2, Lt Col Vinkels

Foreign Technology Division
    ATTN: NIIS Library
    ATTN: TQTD, B. Ballard

Rome Air Development Center
    ATTN: OCS, V. Coyne
    ATTN: TSLD

Rome Air Development Center
    ATTN: EEP, J. Rasmussen

Space Division
    ATTN: YGJB, W. Mercer
    ATTN: YKM, Maj Alexander
    ATTN: YKM, Cpt Norton

Stragetic Air Command
    ATTN: NRT
    ATTN: DCX
    ATTN: XPFS
    ATTN: ADWATE, B. Bauer
    ATTN: DCXT, T. Jorgensen

OTHER GOVERNMENT AGENCIES

Central Intelligence Agency
    ATTN: OSWR/SSD for K. Feuerpfeil
    ATTN: OSWR/NED

Department of Commerce
National Bureau of Standards
    ATTN: Sec Ofc for R. Moore

Department of Commerce
National Oceanic & Atmospheric Admin
    ATTN: R. Grubb

Institute for Telecommunications Sciences
    ATTN: L. Berry
    ATTN: A. Jean
    ATTN: W. Utlaut

NATO

NATO School (SHAPE)
    ATTN: US Documents Officer

DEPARTMENT OF ENERGY CONTRACTORS

EG&G, Inc
    ATTN: D. Wright
    ATTN: J. Colvin

University of California
Lawrence Livermore National Lab
    ATTN: Technical Info Dept Library
    ATTN: L-389, R. Ott
    ATTN: L-31, R. Hager

Sandia National Labs, Livermore
    ATTN: T. Cook
    ATTN: B. Murphey

DEPARTMENT OF ENERGY CONTRACTORS (Continued)

Los Alamos National Laboratory
    ATTN: MS 664, J. Zinn
    ATTN: P. Keaton
    ATTN: D. Simons
    ATTN: MS 670/J. Hopkins
    ATTN: T. Kunkle, ESS-5
    ATTN: R. Jeffries
    ATTN: J. Wolcott
    ATTN: C. Westervelt

Sandia National Lab
    ATTN: D. Dahlgren
    ATTN: Tech Lib 3141
    ATTN: Space Project Div
    ATTN: D. Thornbrough
    ATTN: Org 1250, W. Brown
    ATTN: Org 4231, T. Wright

DEPARTMENT OF DEFENSE CONTRACTORS

Aerospace Corp
    ATTN: V. Josephson
    ATTN: T. Salmi
    ATTN: R. Slaughter
    ATTN: I. Garfunkel
    ATTN: J. Straus
    ATTN: D. Olsen

Analytical Systems Engineering Corp
    ATTN: Radio Sciences

Analytical Systems Engineering Corp
    ATTN: Security

BDM Corp
    ATTN: L. Jacobs
    ATTN: T. Neighbors

Berkeley Research Associates, Inc
    ATTN: J. Workman
    ATTN: S. Brecht
    ATTN: C. Prettie

Boeing Aerospace Co
    ATTN: MS 87-63, D. Clauson

Boeing Co
    ATTN: G. Hall
    ATTN: S. Tashird

Booz-Allen & Hamilton, Inc
    ATTN: B. Wilkinson

BR Communications
    ATTN: J. McLaughlin

University of California at San Diego
    ATTN: H. Booker

Charles Stark Draper Lab, Inc
    ATTN: A. Tetewski
    ATTN: J. Gilmore
    ATTN: D. Cox

Computer Sciences Corp
    ATTN: F. Eisenbarth

DEPARTMENT OF DEFENSE CONTRACTORS (Continued)

Comsat Labs
        ATTN: D. Fang
        ATTN: G. Hyde

Cornell University
        ATTN: D. Farley, Jr
        ATTN: M. Kelly

E-Systems, Inc
        ATTN: R. Berezdivin

Electrospace Systems, Inc
        ATTN: H. Logston
        ATTN: P. Phillips

EOS Technologies, Inc
        ATTN: B. Gabbard

ESL, Inc
        ATTN: R. Ibaraki
        ATTN: R. Heckman
        ATTN: J. Lehman
        ATTN: E. Tsui
        ATTN: J. Marshall

General Electric Co
        ATTN: C. Zierdt
        ATTN: A. Steinmayer

General Electric Co
        ATTN: G. Millman

General Research Corp
        ATTN: B. Bennett

GEO-Centers, Inc
        ATTN: E. Marram

Harris Corp
        ATTN: E. Knick

Honeywell, Inc
        ATTN: G. Collyer, Avionics Dept
        ATTN: G. Terry, Avionics Dept

Horizons Technology, Inc
        ATTN: R. Kruger

HSS, Inc
        ATTN: D. Hanser

IBM Corp
        ATTN: H. Glander

Institute for Defense Analyses
        ATTN: E. Bauer
        ATTN: H. Wolfhard
        ATTN: J. Aein
        ATTN: H. Gates

International Tel & Telegraph Corp
        ATTN: Technical Library

International Tel & Telegraph Corp
        ATTN: G. Wetmore

JAYCOR
        ATTN: J. Sperling

DEPARTMENT OF DEFENSE CONTRACTORS (Continued)

JAYCOR
        ATTN: J. Doncarlos

Johns Hopkins University
        ATTN: J. Newland
        ATTN: T. Evans
        ATTN: P. Komiske
        ATTN: J. Phillips

Kaman Sciences Corp
        ATTN: T. Stephens

Kaman Tempo
        ATTN: B. Gambill
        ATTN: DASIAC
        ATTN: J. Devore
        ATTN: W. Knapp
        ATTN: K. Schwartz
        ATTN: W. McNamara

Litton Systems, Inc
        ATTN: B. Zimmer

Lockheed Missiles & Space Co, Inc
        ATTN: R. Sears
        ATTN: J. Kumer

Lockheed Missiles & Space Co, Inc
        ATTN: C. Old/Dept 68-21
        ATTN: D. Churchill Dept 81-11
        ATTN: Dept 60-12

M.I.T. Lincoln Lab
        ATTN: D. Towle

MA COM Linkabit Inc
        ATTN: H. Van Trees
        ATTN: A. Viterbi
        ATTN: I. Jacobs

Magnavox Govt & Indus Electronics Co
        ATTN: G. White

Martin Marietta Corp
        ATTN: R. Heffner

McDonnell Douglas Corp
        ATTN: W. Olson
        ATTN: Technical Library Services
        ATTN: R. Halprin
        ATTN: H. Spitzer

Meteor Communications Corp
        ATTN: R. Leader

Mission Research Corp
        ATTN: R. Hendrick
        ATTN: C. Lauer
        ATTN: R. Kilb
        ATTN: F. Fajen
        ATTN: R. Bigoni
        ATTN: G. McCartor
        ATTN: F. Guigliano
        ATTN: Tech Library
        ATTN: S. Gutsche
        ATTN: R. Bogusch

Mitre Corp
    ATTN: A. Kymmel
    ATTN: B. Adams
    ATTN: G. Harding
    ATTN: C. Callahan
    ATTN: MS J104 M. R. Dresp

Mitre Corp
    ATTN: W. Hall
    ATTN: M. Horrocks
    ATTN: W. Foster
    ATTN: J. Wheeler

Pacific-Sierra Research Corp
    ATTN: F. Thomas
    ATTN: E. Field, Jr
    ATTN: H. Brode, Chairman SAGE

Pennsylvania State University
    ATTN: Ionospheric Research Lab

Photometrics, Inc
    ATTN: I. Kofsky

Physical Dynamics, In
    ATTN: E. Fremouw

Physical Research, Inc
    ATTN: R. Deliberis

R&D Associates
    ATTN: R. Lelevier
    ATTN: C. Greifinger
    ATTN: R. Turco
    ATTN: H. Ory
    ATTN: W. Wright
    ATTN: M. Gantsweg
    ATTN: W. Karzas
    ATTN: F. Gilmore

R&D Associates
    ATTN: B. Yoon

Rand Corp
    ATTN: E. Bedrozian
    ATTN: C. Crain

Riverside Research Institute
    ATTN: V. Trapani

Rockwell International Corp
    ATTN: R. Buckner

Rockwell International Corp
    ATTN: S. Quilici

Santa Fe Corp
    ATTN: D. Paolucci

Science Applications, Inc
    ATTN: L. Linson
    ATTN: C. Smith
    ATTN: E. Straker
    ATTN: D. Hamlin

Science Applications, Inc
    ATTN: J. Cockayne

SRI International
    ATTN: G. Price
    ATTN: R. Tsunoda
    ATTN: W. Chesnut
    ATTN: R. Livingston
    ATTN: D. Neilson
    ATTN: J. Petrickes
    ATTN: D. McDaniels
    ATTN: M. Baron
    ATTN: R. Leadabrand
    ATTN: A. Burns
    ATTN: C. Rino
    ATTN: G. Smith
    ATTN: V. Gonzales
    ATTN: W. Jaye
4 cy ATTN: J. Vickrey

Stewart Radiance Laboratory
    ATTN: J. Ulwich

Sylvania Systems Group
    ATTN: R. Steinhoff

Sylvania Systems Group
    ATTN: J. Concordia
    ATTN: I. Kohlberg

Technology International Corp
    ATTN: W. Boquist

Tri-Com, Inc
    ATTN: D. Murray

TRW Electronics & Defense Sector
    ATTN: G. Kirchner
    ATTN: R. Plebuch
    ATTN: D. Dee

Utah State University
    ATTN: A. Steed
    ATTN: D. Burt
    ATTN: L. Jensen, Elec Eng Dept
    ATTN: K. Baker, Dir Atmos & Space Sci

Visidyne, Inc
    ATTN: C. Humphrey
    ATTN: O. Shepard
    ATTN: W. Reidy
    ATTN: J. Carpenter